

## **Laser-based assessment of road aggregate particle shape and texture properties with the aim of deriving comparative models**

- I.J. Breytenbach

Pr. Sci. Nat.

SAICE Visitor

Tel: 082 577 6215

Fax: (012) 9912 555

E-mail: [soilkraft02@iburst.co.za](mailto:soilkraft02@iburst.co.za)

Postal Address: PO Box 73478, Lynnwood Ridge, 0040

- Dr J.K. Anochie-Boateng

SAICE Visitor

Tel: (012) 841 2947

Fax: (012) 841 2690

E-mail: [JAnochieBoateng@csir.co.za](mailto:JAnochieBoateng@csir.co.za)

Postal Address: CSIR Built Environment, Building 2C, PO Box 395, Pretoria,  
0001

- Dr P. Paige-Green

Natural Scientist

(Member, SAICE)

Tel: 082 444 1121

Fax: (012) 345 6028

E-mail: [paigegreenconsult@gmail.com](mailto:paigegreenconsult@gmail.com)

Postal Address: Postnet Suite #89, Private Bag X8, Elardus Park, 0047

o Prof J.L. van Rooy

Pr. Sci. Nat.

Tel: (012) 420 2023

Fax: (012) 362 5219

E-mail: [louis.vanrooy@up.ac.za](mailto:louis.vanrooy@up.ac.za)

Postal Address: Department of Geology, University of Pretoria, Private Bag

X20, Hatfield,

0028.

**Keywords/terms:** Road aggregate, particle shape, particle texture, laser scanner, particle model

## **ABSTRACT**

Research was undertaken using an innovative three dimensional (3D) laser scanning tool to study the shape and texture characteristics of road aggregate particles. Aggregate materials used for road construction, including G1 crushed rocks of different geological origins, recycled aggregate, and alluvial gravel (not used as aggregate) were used for this study. Representative samples were scanned using the laser system to collect 3D aggregate data for analyses and subsequently, develop comparative models.

The objective was to arrange the aggregate particles in a sequence based on their surface texture. Two models were proposed and key aspects evaluated against each

other. Ultimately, one model was selected that may be improved and used for further research. The study found that while it is possible to use the 3D aggregate scan data to produce comparative models, distinguishing between particle shape and texture proved a daunting task and that particle elongation must be considered as a major influencing factor.

## **INTRODUCTION**

The study forms part of a PhD research (Breytenbach, 2013), which is aimed at deriving a tabulated range of particles that could graphically or numerically represent a range of aggregate shape and texture properties. . The proposed model, if validated , should be able to arrange particles in a certain sequence based on the texture properties. The method would lend scientific substantiation to particle shape characterisation instead of visual observations, which have previously (to a larger extent ) used to quantify aggregate particle shape and texture.

An innovative study using three dimensional laser scanning technology in the application of road materials is under development at CSIR. The laser scanning method is applied to road construction aggregate using different approaches, attempting to study aggregate particle properties in great detail and for different applications. Emphasis has thus far been placed on particle shape and surface properties (Anochie-Boateng *et al.*, 2010) and the flakiness index (Anochie-Boateng *et al.*, 2011a) amongst others.

In this paper, the laser scanning method was applied in an attempt to refine the description of particle textures and shapes through two comparative proposed models considering that these models seek to sort aggregate particle data obtained from coarse/angular to smooth/rounded particles.

## **EXISTING METHODS**

A number of advanced methods have been applied to study particle shape properties of aggregates. Rao *et al.* (2002) attempted to quantify the angularity of particles and ultimately showed that their approach (using image analysis) could distinguish between rounded gravel and crushed stone. Fletcher *et al.* (2002) discuss an aggregate imaging system (AIMS), using a back-lit system. It is clear that this method is able to determine the angularity of coarse and fine aggregate, as well as relative dimensions, thereby enabling the identification of flat or elongated particles. Other back-lit systems have also been used (Fernlund, 2005; Ken *et al.*, 2009), while Descantes *et al.* (2006) and Bouquety *et al.* (2006) used videographers in combination with a backlit system.

Kim *et al.* (2003) analysed materials using a laser-based approach. The digital image technology (DIT) calculates the volume of a particle, as well as the minimum square aperture through which a particle could fit.

However, the approaches discussed above are based on imaging techniques, which could at best capture two dimensional (2D) physical attributes of the aggregate

particles. In reality, aggregate particles are three dimensional; accordingly any improved techniques or methods should be able to address the physical properties in three dimensions.

The approach used in this research is based on 3D scanning techniques which were recently introduced by the CSIR (Anochie-Boateng *et al.*, 2010; Anochie-Boateng *et al.*, 2011a; Anochie-Boateng *et al.*, 2011b). Details will not be repeated in this paper.

## **METHODOLOGY**

### **Scanning Procedure**

Scanning of aggregate particles is done according to a protocol developed specifically for the laser scanner at the CSIR (Anochie-Boateng and Komba, 2010). The approach adopted consists of four steps which can be summarised as follows:

1. Scanning: The first step entails physical processing of the particle by means of scanning. During the first phase scanning four faces of a particle, which is placed on a rotating table in the scanner, are scanned. The particle is then rotated in order to scan the remaining two faces which were not in line of sight during the first scan phase (i.e. top and bottom).
2. Alignment: During this step the data obtained from the two scanning phases are orientated by the user. In essence this step simply rotates and moves the two scan dataset into the correct orientation relative to each other.
3. Combining: Software is used to combine the correctly orientated data.

4. Merging: The combined data is merged into a single object and saved as a single particle presented in three dimensions. Any refinement (e.g. removal of small imperfections or overlapping areas etc.) is also executed during this step.

The scanning density used by the scanning equipment can be varied according to the user's requirements. The density used affects the resolution of the final result and also the amount of time required to scan the particle. A higher scan resolution results in longer scan time. The maximum scan resolution of the equipment is 0.1mm. The time required to scan a particle is also affected by the size of a particle.

### **Particle Selection**

The aggregate particles and materials used during this study is part of other on-going projects running congruently at the CSIR. The sourced aggregates used in this study included the following geological materials:

- Quartzite (G1 aggregate from stockpile) – Magaliesberg Formation, Pretoria Group, collected in Pretoria, Gauteng
- Granite (G1 aggregate from stockpile) – Johannesburg Dome, collected in Midrand, Gauteng
- Tillite (G1 aggregate from stockpile) – Dwyka Group, Karoo Supergroup, collected in Verulam, Kwazulu-Natal
- Hornfels (G1 aggregate from stockpile) – Tygerberg Formation, Malmesbury Group, collected in Durbanville, Western Cape

- Dolerite (G1 aggregate from stockpile) – Karoo Supergroup, collected in Trichardt, Mpumalanga
- Recycled aggregate – National Asphalt plant in Durban, Kwazulu-Natal
- Alluvial gravel – Quaternary aged surface deposit sampled from the river bed of the Molopo River, some 120km west of Mafikeng, North West. This material is not an aggregate source

Each material was screened (using a sieve stack) into different particle sizes, for the purposes of scanning. The bulk samples were screened into the +26.5 mm, +19.0 mm, +13.2 mm, +9.5 mm, +6.7 mm and +4.75 mm constituents. Particles of 37.5 mm size and larger were not considered as they fall outside the COLTO (1998) specification for G1 crushed rock aggregate. Particles smaller than 4.75 mm were not scanned due to practical limitations of the scan device.

Once bulk samples were graded into its fractions, 30 particles were selected from each size constituent of each material. Table 1 summarises the number of particles used. In a number of materials the 26.5mm size fraction had some shortages, as the materials were shared with other research projects. After selection, the particles were cleaned and oven-dried (at 105°C for 24 hours) and left to cool before being scanned.

**[Insert Table 1 here]**

## **Data Capture**

Scan data are captured in a spread sheet format and was entered manually into Microsoft Excel®. The final result was six spread sheets (i.e. 26.5 mm, 19.0 mm, 13.2 mm, 9.5 mm, 6.7 mm and 4.75 mm) which contained data of all material types scanned.

Parameters that were recorded in the dataset include the material type, the number of the sample particles and the three primary dimensions (i.e. length, width and depth/height). The volume ( $\text{mm}^3$ ) and total surface area ( $\text{mm}^2$ ) of each particle was recorded directly from the scan results. The scan data and/or spread sheets could not be included in this article due to its volume (i.e. 1149 data sets).

## **DISCUSSION**

Two working concept models were developed using the scan data, one of which was ultimately abandoned as the model was heavily affected by factoring in the so-called elongation value (the ratio between the minimum and maximum dimensions of a particle). The second model proved to be superior to the first in that it discerned between differences in particle textures, as opposed to being excessively affected by the particle shape. The second model was further refined to develop a reference system for each particle size to enable comparison of particle textures.

## **Data Manipulation**



The data arrangement described above was done specifically with the aim of calculating another parameter to be used in analysis. In spread sheet form the parameter was labelled “Elongation Value”. The flakiness index has previously been assessed using this same laser scanning system by Anochie-Boateng *et al.* (2011) but the approach adopted here (i.e. using the elongation value) simplified data analysis considerably.

In order to make provision for the effects of elongated or flattened particle shapes, data were divided into subgroups to assess whether the elongation/flatness would affect the derived model(s). It was therefore necessary to derive a descriptor for its assessment. Particle data were divided into “regular” and “elongated” subsets, based on the ratio between the maximum and minimum dimensions of a particle. An “*elongation value*” was calculated as follows:

$$EV = \frac{Length}{Depth} \quad (1)$$

where

*EV* = Elongation Value

*Length* = the particle’s maximum dimension

*Depth* = the particle’s minimum dimension

Particles with an  $EV > 2$  were considered to be “elongated” while particles with  $EV < 2$  were considered to be “regular”. Spread sheet data were sorted based on the calculated elongation values and subdivided accordingly. Once data sorting had been completed, limited descriptive statistics and histogram analyses were done to verify data properties and identify potential shortages in data ranges.

Data were processed for all particle sizes and subsequently two comparative models, one for elongated particles and one for regular particles, and were produced for each size fraction.

### **Proposed Model One**

The first model considers three parameters, namely particle volume, particle surface area and the calculated elongation value. The *model value* is calculated as follows:

$$\text{Model value} = \frac{V}{A} \times EV \quad (2)$$

where

$V$  = particle volume ( $\text{mm}^3$ )

$A$  = particle surface area ( $\text{mm}^2$ )

$EV$  = elongation value

Histogram analyses for the regular and elongated data sets are illustrated in Figure 1 and Figure 2, respectively. From the elongated particles histogram (Figure 2) it is clear that there are no data for the model value range between 6.0 and 7.0, which produced gaps in the output chart for the model. This underlines the effects of factoring in the elongation value and the limitations it imposes on the derived models.

**[Insert Figure 1 here]**

**[Insert Figure 2 here]**

After revision of the histogram data, model values were sorted in ascending order and model value ranges were calculated. Ten random values within the data range were selected and the closest corresponding particle was entered into a table. Table 2 shows the models selected for elongated particles, while Table 3 shows the models selected for regular particles.

**[Insert Table 2 here]**

**[Insert Table 3 here]**

The tabular results reflect the findings of the histogram analyses where gaps were found in the data range proposed for the elongated particles. The effects of factoring the elongation value into the model also introduced a bias towards elongated particles in both datasets. Subsequently the results show little refinement in data, particularly for the elongated particles. Considering that the aim of the model was to sort the particle data from coarse/angular to smooth/rounded particles, it is clear that this model was only moderately successful for regular particles and largely unsuccessful for elongated particles.

### **Proposed Model Two**

The results from the first model led to the second model, where the elongation value is no longer factored into the model value:

$$Model\ value = \frac{V}{A} \tag{3}$$

$V$ , and  $A$  are defined in Equation 2.

The subsequent histogram analyses show an improvement in model data presentation. While the histogram for regular particles (Figure 3) shows little improvement over the same dataset for model one, the histogram for elongated particles (Figure 4) no longer has the previous gap in data for the second model.

**[Insert Figure 3 here]**

**[Insert Figure 4 here]**

The calculated model values were again sorted in ascending order. Ten equal increments were identified between the minimum and maximum data values. The data sets were used to identify the nearest corresponding value and the applicable particle was again entered into a table. The results are summarised in Table 4 while Table 5 and Table 6 show the results for elongated and regular particles, respectively.

**[Insert Table 4 here]**

**[Insert Table 5 here]**

**[Insert Table 6 here]**

In this instance the results showed significant refinement based on the second model data. The refinement is perhaps more clearly observed in the elongated particle results than in the regular particle results. Model two shows good potential to arrange particles from rough/angular to smooth/rounded, although there is still room for improvement.

## **Model Comparison**

By comparing the results from the two proposed models visually, it is clear that the second model refines and arranges data more effectively from rough or angular particles to smooth or rounded particles. The limited calculated model data in model one may be due to factoring the elongation value into the calculations.

## **CONCLUSION**

The research was undertaken to determine if a three dimensional laser-based scanning method can be applied to the modelling of shape and texture of road aggregate particles in an attempt to arrange particles based on their surface texture. The laser technique applied was relatively successful to produce comparative models that can be used to describe or classify aggregate particle shape and surface texture properties. Scan data obtained from scanning of various aggregate materials were used to develop and compare two derived models.

The results indicate that the proposed model 2 shows potential to better describe the shape and surface texture properties of the aggregates when compared to model 1 although further development is required. It was found that factoring an elongation value (*EV*) into the proposed model 1 had negative effect. The data with the elongation value were heavily biased towards the inclusion of either elongated or flat particles. Generally, none of the proposed models could effectively discern between particle roughness and angularity as the two parameters appear to be strongly co-dependant.

## **RECOMMENDATIONS**

It is suggested that the approach used in model two be considered for further analyses and investigations of particle properties. Additional scan data obtained from mixed geological sources will also assist in the further refinement of the models. Further studies may have to investigate how elongation factor can be combined with surface area or volume separately as alternatives.

## **ACKNOWLEDGEMENTS**

Work presented in this paper received funding from Council for Scientific and Industrial Research (CSIR) strategic research panel (SRP) project TA 2001-001. The authors would like to acknowledge the CSIR R&D office for funding this SRP project. Mr Julius Komba of CSIR and University of Pretoria, and Ms Sibongiseni Lusawana of CSIR and Tshwane University of Technology in Pretoria assisted in the scanning of the aggregates used in this paper.

## **REFERENCES**

Anochie-Boateng, J. and Komba, J. (2010). Laser scanning protocol for determining aggregate shape and surface properties, Report number CSIR/BE/IE/IR/2010/0061/B

Anochie-Boateng, J. and Komba, J.J., Mukalenga, N. and Maharaj, A. (2010). *Evaluation of 3D laser device for characterizing shape and surface properties of aggregates used in pavements*. 29<sup>th</sup> Southern Africa Transportation Conference, Pretoria, August 2010

Anochie-Boateng, J., Komba, J., O'Connell, J. (2011a). *Laser-based approach for determining flakiness index of aggregates used in pavements*. 30<sup>th</sup> Southern Africa Transportation Conference, Pretoria, South Africa, July 2011

Anochie-Boateng, J., Komba, J and G.M. Mvelase (2011b). *Advanced and Automated Laser-based Technique to Evaluate Aggregates*. IRF International Road Congress “Innovation in Road Infrastructure”, November 2011, Moscow, Russia.

Bouquety, M.N., Descantes, Y., Barcelo, L., de Larrard, F. and Clavaud, B. (2006). Automated measurement of aggregate properties: Part 2 – flakiness index. *Materials and Structures*, **39**(1), 13 – 19

Breytenbach I.J. (2013). *The Effects of Particle Shape and Texture Characteristics on Shear Properties of Compacted Crushed Stone Aggregate Used in Road Construction*. Unpublished PhD thesis, University of Pretoria, South Africa

COLTO (Committee of Land Transport Officials) (1998). Standard Specifications for Road and Bridge Works for State Road Authorities. South African Institute of Civil Engineers (SAICE)

Descantes, Y., Fosse, Y. and Ehret, G. (2006). Automated measurement of aggregate properties: Part 1 – Crushed and broken surfaces in coarse aggregate particles. *Materials and Structures*, **39**(1), 3 – 12

Fernlund, J.M.R. (2005). Image analysis method for determining 3-D size distribution of coarse aggregates. *Bulletin of Engineering Geology and the Environment*, **64**(2), 159 - 166

Fletcher, T., Chandan, C., Masad, E. and Sivakumar, K. (2002). *Aggregate Imaging System (AIMS) for Characterizing the shape of Fine and Coarse Aggregate*. A paper submitted to the 82<sup>nd</sup> Annual Transportation Research Board for presentation and presentation, submitted July 2002

Ken, C., Pan, Z. and Xuemei, Z. (2009). A description method for arbitrarily shaped and sized granules in 2D image. *Journal of Electronics (China)*, **26**(3), 423 – 427

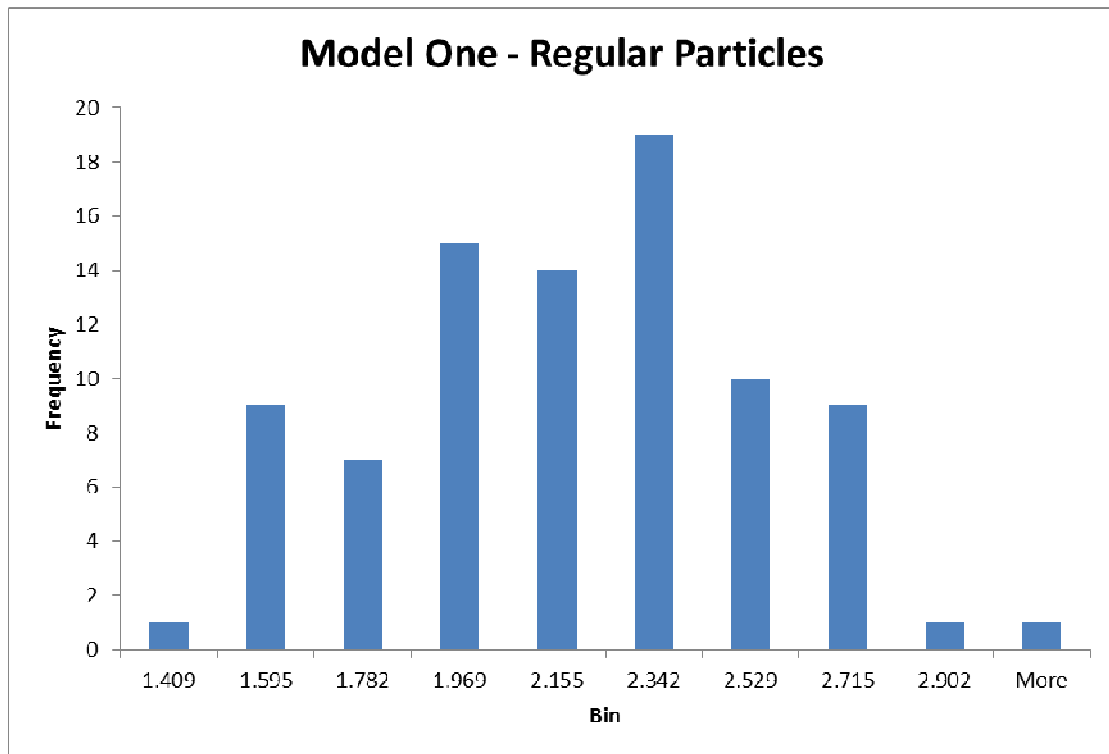
Kim, H., Haas, C.T. and Rauch, A.F. (2003). 3D Image Segmentation of Aggregates from Laser Profiling. *Computer-Aided Civil and Infrastructure Engineering*, **18**(4), 254 - 263

Rao, C., Tutumluer, E. and Kim, I.T. (2002). *Quantification of Coarse Aggregate Angularity based on Image Analysis*. Transportation Research Record, No. 1787, TRB, National Research Council, Washington D.C., pp. 117 – 124

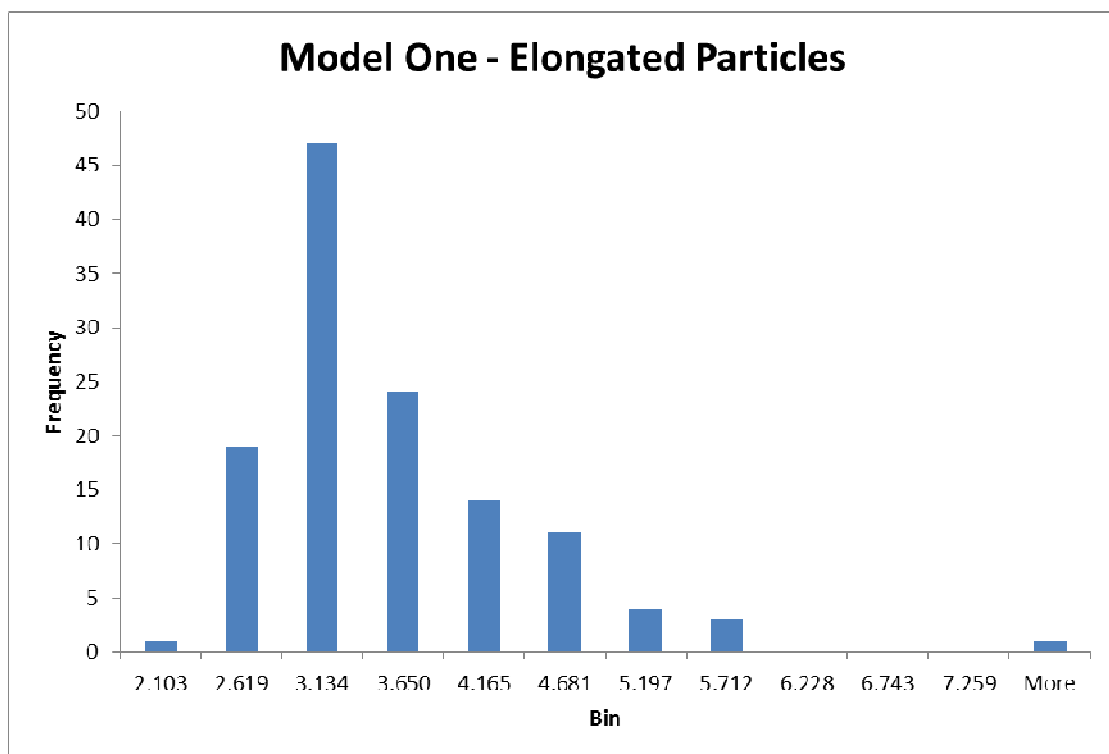


**Table 1** Summary of Scanned Particles

	<b>Quartzite</b>	<b>Granite</b>	<b>Tillite</b>	<b>Hornfels</b>	<b>Recycled Aggregate</b>	<b>Alluvial Gravel</b>	<b>Dolerite</b>	<b>Total</b>
<b>26.5mm</b>	-	22	30	18	-	-	30	100
<b>19.0mm</b>	30	30	30	30	30	30	30	210
<b>13.2mm</b>	30	30	30	30	30	30	30	210
<b>9.5mm</b>	30	30	30	30	30	30	30	210
<b>6.7mm</b>	30	30	30	30	30	30	30	210
<b>4.75mm</b>	30	30	30	30	30	30	29	209
<b>Total</b>	150	172	180	168	150	150	179	<b>1149</b>

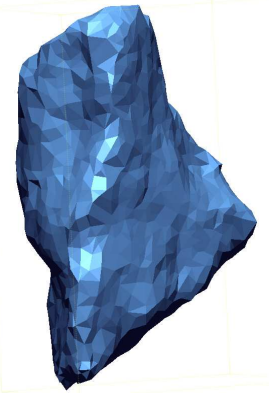
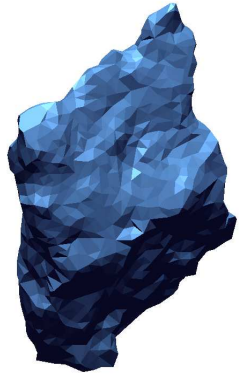
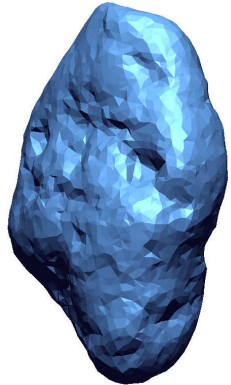
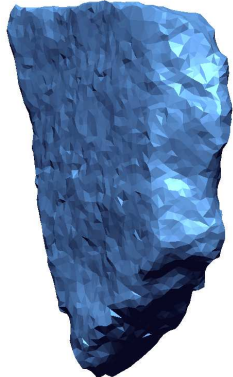
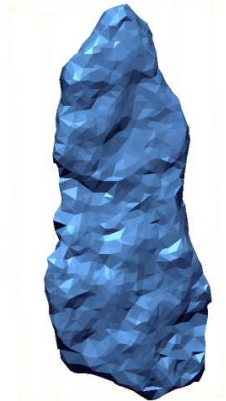
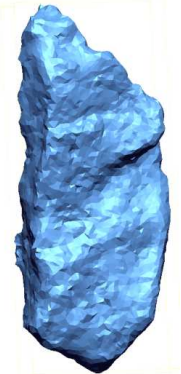

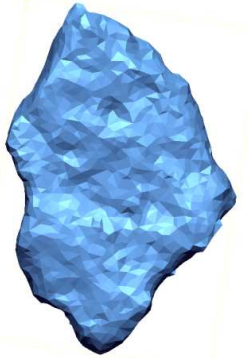


**Figure 1** Histogram for model one output data - regular particles

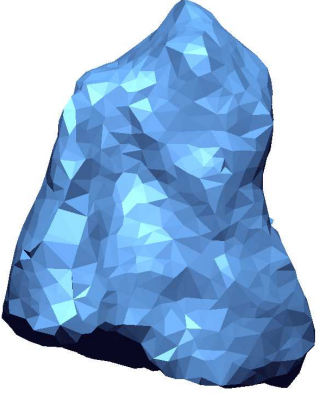
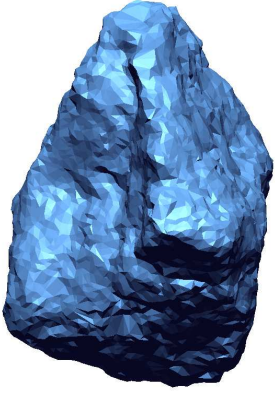

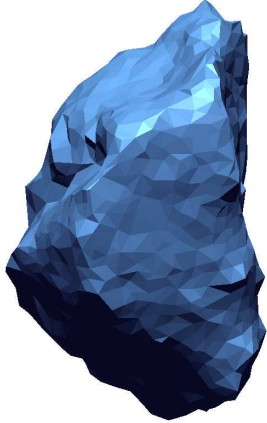
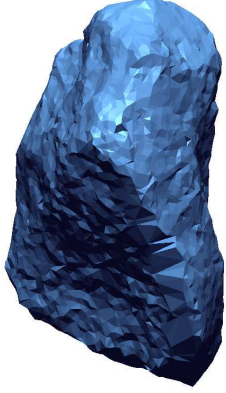
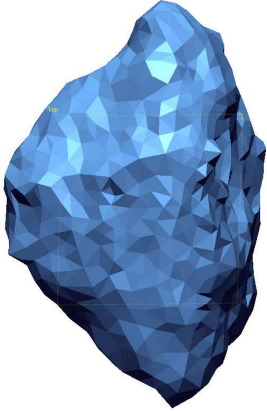
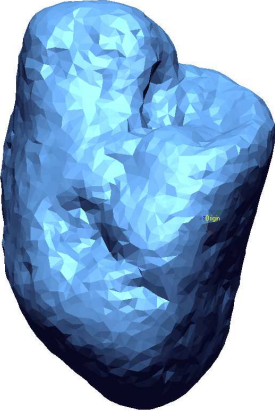
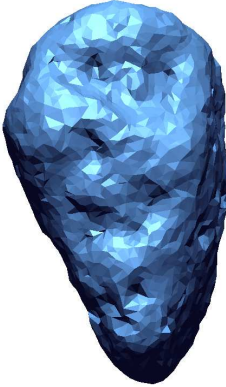
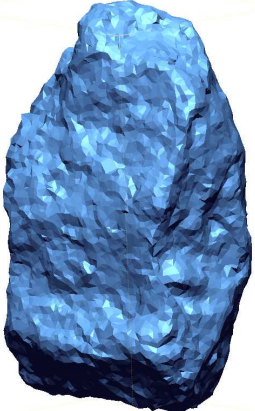
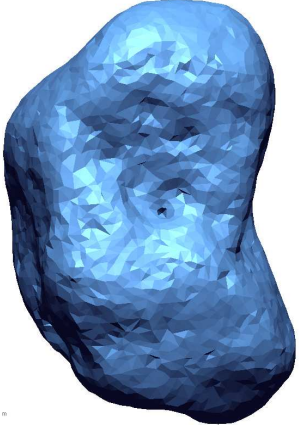


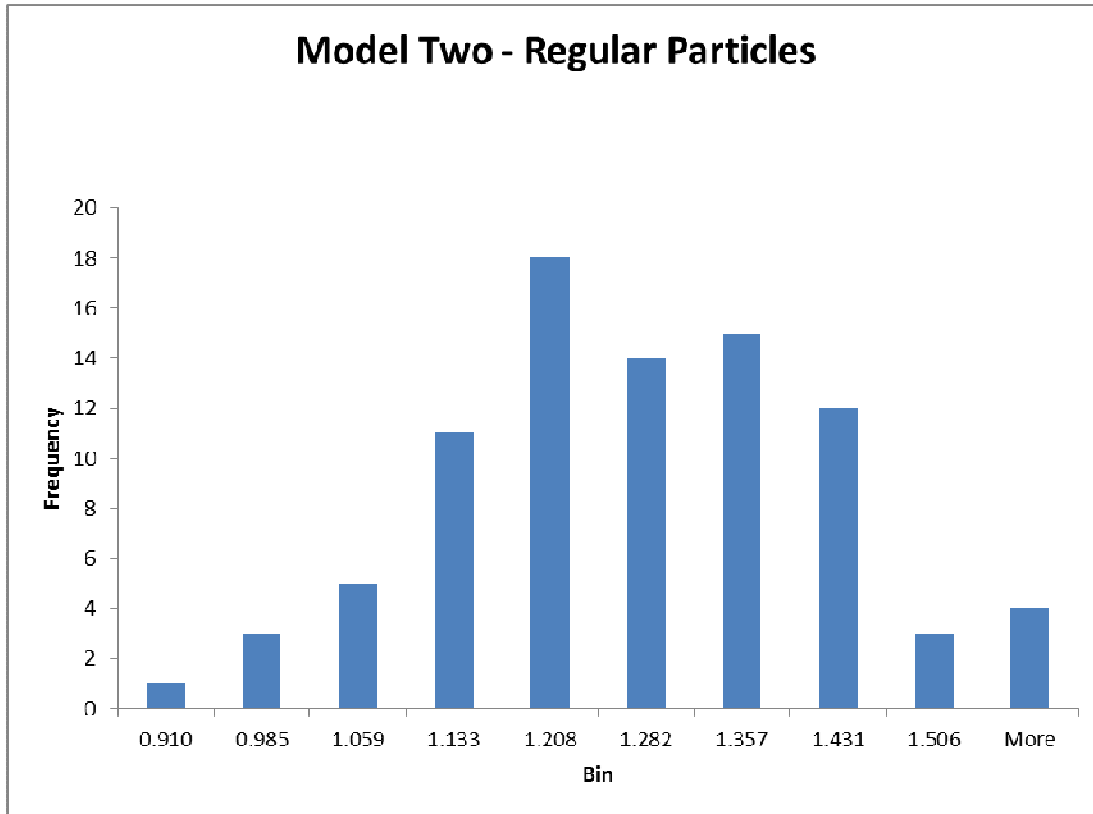
**Figure 2** Histogram for model one output data - elongated particles

**Table 2** Elongated 6.7mm particles – model one

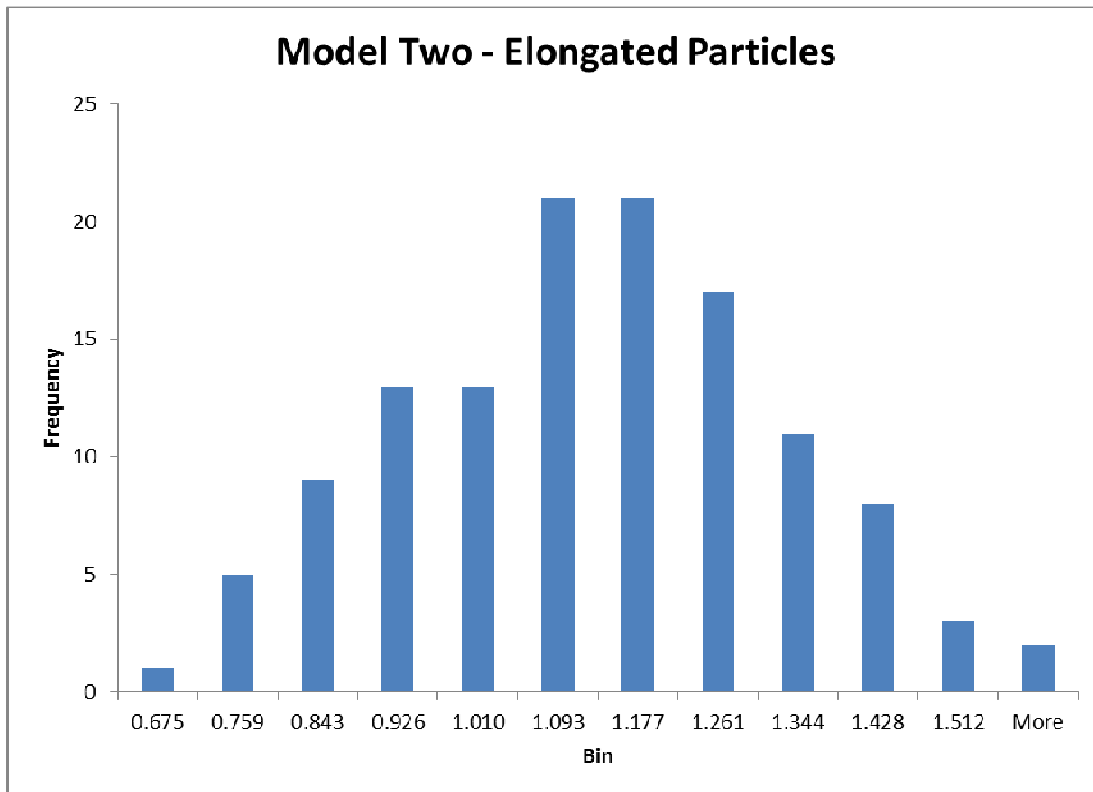
 <p><b>2.103</b> (Hornfels 16)</p>	 <p><b>2.736</b> (Dolerite 11)</p>	 <p><b>3.345</b> (Gravel 21)</p>	 <p><b>4.000</b> (Hornfels 24)</p>	 <p><b>4.630</b> (Granite 28)</p>
 <p><b>5.433</b> (Quartzite 29)</p>	 <p><b>5.600</b> (Quartzite 28)</p>	<p>(Insufficient data)</p>	<p>(Insufficient data)</p>	 <p><b>7.775</b> (Tillite 28)</p>

**Table 3** Regular 6.7mm particles – model one

 <p><b>1.409</b> (Tillite 10)</p>	 <p><b>1.584</b> (Granite 9)</p>	 <p><b>1.782</b> (Hornfels 9)</p>	 <p><b>1.965</b> (Tillite 1)</p>	 <p><b>2.154</b> (Quartzite 18)</p>
 <p><b>2.322</b> (Recycled Aggregate 1)</p>	 <p><b>2.541</b> (Gravel 23)</p>	 <p><b>2.706</b> (Gravel 19)</p>	 <p><b>2.774</b> (Granite 12)</p>	 <p><b>3.089</b> (Gravel 28)</p>



**Figure 3** Histogram for model two output data - regular particles




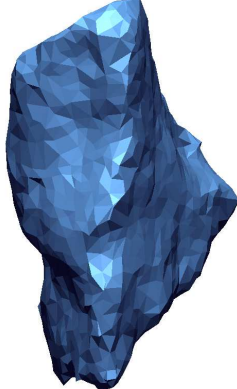

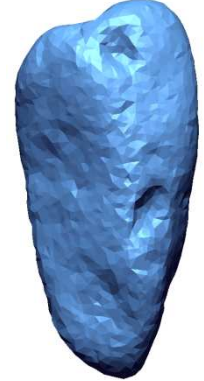



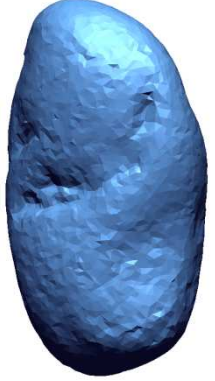


**Figure 4** Histogram for model two output data - elongated particles



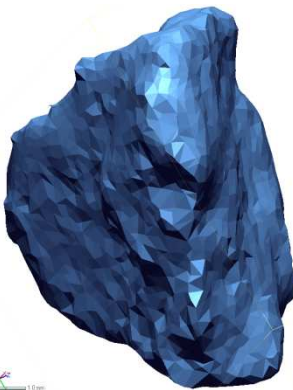
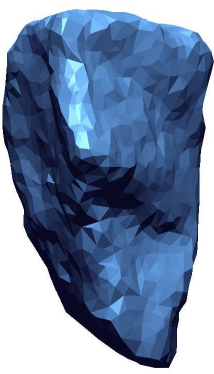
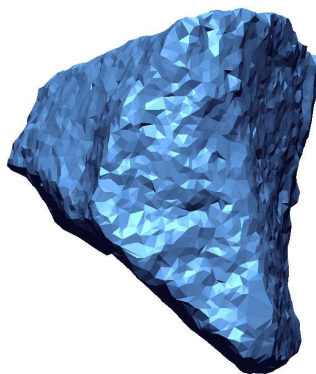

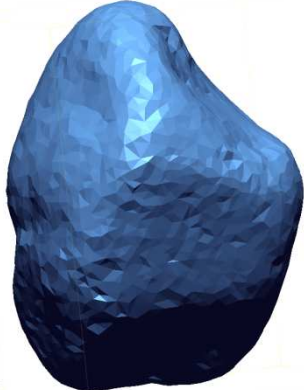

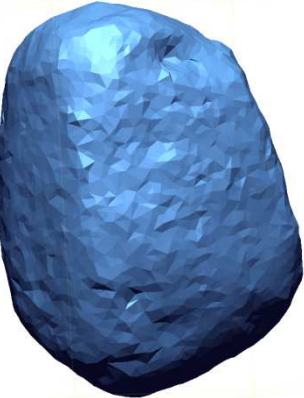
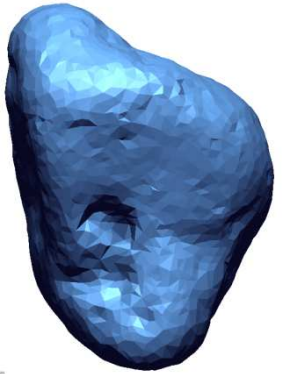
**Table 4** Particle selection for 6.7mm – model two

<b>REGULAR PARTICLES</b>		
<b>Minimum V/A</b>	0.910	
<b>Maximum V/A</b>	1.580	
<b>Range</b>	0.670	
<b>Increments Calculated</b>	0.074	
<b>Increment Value</b>	<b>Nearest Match</b>	<b>Sample/Particle Number</b>
0.910	0.910	Hornfels 10
0.985	0.981	Hornfels 7
1.059	1.062	Tillite 9
1.134	1.139	Tillite 15
1.208	1.208	Quartzite 2
1.282	1.285	Granite 6
1.357	1.354	Gravel 4
1.431	1.439	Gravel 19
1.506	1.513	Gravel 5
1.580	1.580	Gravel 22
<b>ELONGATED PARTICLES</b>		
<b>Minimum V/A</b>	0.675	
<b>Maximum V/A</b>	1.595	
<b>Range</b>	0.920	
<b>Increments Calculated</b>	0.102	
<b>Increment Value</b>	<b>Nearest Match</b>	<b>Sample/Particle Number</b>
0.675	0.675	Hornfels 30
0.778	0.774	Tillite 26
0.880	0.873	Granite 27
0.982	0.981	Hornfels 16
1.084	1.084	Quartzite 15
1.186	1.182	Gravel 25
1.289	1.284	Dolerite 8
1.391	1.379	Dolerite 30
1.493	1.490	Recycled Aggregate 12
1.595	1.595	Gravel 29

**Table 5** Elongated 6.7mm particles – model two

 <p><b>0.675</b> (Hornfels 30)</p>	 <p><b>0.774</b> (Tillite 26)</p>	 <p><b>0.873</b> (Granite 27)</p>	 <p><b>0.981</b> (Hornfels 16)</p>	 <p><b>1.084</b> (Quartzite 15)</p>
 <p><b>1.182</b> (Gravel 25)</p>	 <p><b>1.284</b> (Dolerite 8)</p>	 <p><b>1.379</b> (Dolerite 30)</p>	 <p><b>1.490</b> (Recycled Aggregate 12)</p>	 <p><b>1.595</b> (Gravel 29)</p>

**Table 6** Regular 6.7mm particles – model two

 <p><b>0.910</b> (Hornfels 10)</p>	 <p><b>0.981</b> (Hornfels 7)</p>	 <p><b>1.062</b> (Tillite 9)</p>	 <p><b>1.139</b> (Tillite 15)</p>	 <p><b>1.208</b> (Quartzite 2)</p>
 <p><b>1.285</b> (Granite 6)</p>	 <p><b>1.354</b> (Gravel 4)</p>	 <p><b>1.439</b> (Gravel 19)</p>	 <p><b>1.513</b> (Gravel 5)</p>	 <p><b>1.580</b> (Gravel 22)</p>